

# Design and Operational Aspects of All-Electric Thruster Control Systems for Geostationary Satellites

Marshall H. Kaplan\*

*The Pennsylvania State University, University Park, Pa.*

Results of an all-electric thruster control concept study for geostationary satellites are presented. Early work on this type of system emphasized feasibility rather than design and operational aspects. Conservative estimates of 1975 technology were used as guides in selecting possible thruster combinations and component sites to satisfy basic mission requirements and constraints. The present work goes beyond 1975 technology to that of the late 1970's and considers innovations in hardware and operational techniques which may permit significant reductions in control system weight and components. Finally, recommendations regarding thruster development and satellite design compatible with optimum all-electric control systems are offered. It is concluded that, for systems without momentum wheels or gyros, three orthogonal components of control torque and continuous yaw sensing are required to ensure a stable automatic control system. Furthermore, alternating use of different inclination control thrusters will be highly desirable if these thrusters are canted away from the orbit normal direction due to plume impingement problems.

## Introduction

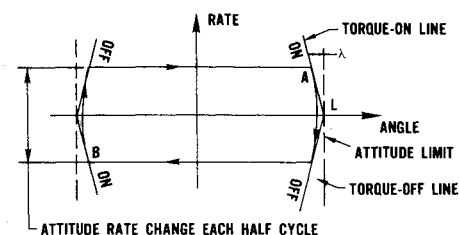
THE expression "all-electric thruster control" is used to describe the technique of actively controlling the orbit and attitude of a nonspinning satellite without using momentum exchange devices, i.e., momentum wheels or control moment gyros. Thus, mass expulsion devices are assumed for generation of control torques. The fundamental control system considered here consists of continuous-mode-type thrusters for inclination control and the ability to apply attitude torques via pulsed-mode devices or techniques. For example, electron-bombardment thrusters might be good candidates for north-south functions, and Teflon pulsed-plasma thrusters might be considered for attitude torque application. Each application to be discussed may require different thruster properties, and these are specified in each case.

The work presented here represents results of further study of the all-electric thruster control concept for geostationary satellites proposed in Ref. 1. As opposed to early efforts on this type of system, which emphasized feasibility, this work considers hardware innovations and operational techniques that may permit significant reductions in control system weight and components. Specific areas studied include duty cycle analysis, minimum thruster component configurations, attitude acquisition sequences, and automatic attitude control requirements. Operational techniques to minimize special problems such as impingement and orbital dynamics coupling effects that arise from inclination control are also described. In addition, attitude control schemes using orbit control thrusters are discussed as representatives of possible future development goals associated with optimization of overall control systems. Interactions between propellant usage, duty cycles, and impulse bit size are considered and applied to practical situations. Finally, recommendations regarding

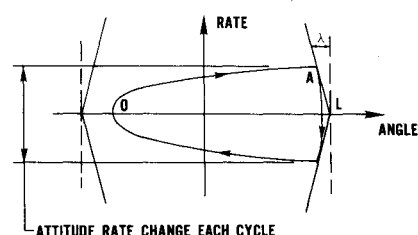
thruster development and satellite design compatible with optimum, all-electric control systems are proposed.

## Duty Cycle Analysis

It has been argued that the exclusive use of thrusters for attitude control is expensive in terms of propellant mass, especially if accurate orientation control is necessary. This is true of chemical reaction systems because hard-limit cycles are required and specific impulse is low. However electric thrusters offer much smaller repeatable impulse bits at very high specific impulses. Thus, soft-limit cycles are possible, and overall mass may be comparable to that of momentum exchange systems. Therefore, the minimum reproducible impulse bit generated in torque is a primary consideration in comparing control systems. For given attitude holding requirements and perturbing torques associated with a specific satellite, the type of limit cycle control (soft or hard) required is determined by the impulse bit sizes of the thrusters. A hard-limit cycle is shown on the phase plane of Fig. 1a. Thrust is applied at both sides of the prescribed angular limit because the perturbing torque is zero or much smaller than the reaction torque.



a) Hard-Limit Cycle



b) Soft-Limit Cycle

Fig. 1 Phase plane diagram of limit cycles.

Received March 3, 1975. Presented as Paper 75-376 at the AIAA 11th Electric Propulsion Conference, New Orleans, La., March 19-21, 1975; revision received June 5, 1975. The material reported here is based upon work performed under the sponsorship of the International Telecommunications Satellite Consortium (INTELSAT). Views expressed herein are not necessarily those of INTELSAT. The author acknowledges his appreciation to B. Free and G. Hudson of COMSAT Labs. for their helpful suggestions and discussions.

Index categories: Electric and Advanced Space Propulsion; Spacecraft Attitude Dynamics and Control; Spacecraft Propulsion Systems Integration.

\*Associate Professor of Aerospace Engineering. Associate Fellow AIAA.

Figure 1b shows a soft-limit cycle which requires thrust at only one extremity. This cycle is permissible when the disturbing torques are large enough to decelerate the vehicle and reverse its direction before reaching the other limit. If the minimum impulse bit of a system can be controlled so that a soft-limit cycle is the normal mode of operation, orientation is controlled at a minimum propellant cost. Coupled with high specific impulse, this efficient propellant utilization makes electric thrusters primary candidates for attitude control actuators. Torque impulse can be applied by a specific pulsed-mode device or by pulsing the beam deflection function of a continuous-type thruster.

For the duty cycle, analysis, coupling between axes may be ignored. Torque component equations are

$$T_X = I_X \ddot{\phi}, \quad T_Y = I_Y \ddot{\theta}, \quad T_Z = I_Z \ddot{\psi} \quad (1)$$

where  $T_X$ ,  $T_Y$ , and  $T_Z$  are torque components, and  $\phi$ ,  $\theta$ , and  $\psi$  are roll, pitch, and yaw, respectively. These equations can be integrated and solved for rates at the attitude error limits. The required corrective impulses are taken as those which reverse the sign of the rate

$$I_{m\phi} \triangleq \int F_\phi \ell_\phi dt = -2I_X \dot{\phi}_A \quad (2a)$$

$$I_{m\theta} \triangleq \int F_\theta \ell_\theta dt = -2I_Y \dot{\theta}_A \quad (2b)$$

$$I_{m\psi} \triangleq \int F_\psi \ell_\psi dt = -2I_Z \dot{\psi}_A \quad (2c)$$

where  $F_\phi$ ,  $F_\theta$ , and  $F_\psi$  are attitude thrust levels, and  $\ell_\phi$ ,  $\ell_\theta$ , and  $\ell_\psi$  are corresponding moment arms. Thus, force impulses are defined simply as time integrals of the thrust components and are obtained by dividing each of equations (2) by its respective moment arm. The value of  $\lambda$  in Fig. 1 is a function of attitude thrust level. For the case of interest here,  $\lambda$  is extremely small and can be taken as zero. To ensure that attitude accuracy is maintained, the limits of attitude for the soft-limit cycle are assumed to be

$$\phi(t_A) = 0.9 \phi_{\max}, \quad \phi_0 = -0.75 \phi_{\max} \quad (3a)$$

$$\theta(t_A) = 0.9 \theta_{\max}, \quad \theta_0 = -0.75 \theta_{\max} \quad (3b)$$

$$\psi(t_A) = 0.9 \psi_{\max}, \quad \psi_0 = -0.75 \psi_{\max} \quad (3c)$$

to avoid the effects of sensor resolution limits and other uncertainties. If the overall beam pointing requirement is  $0.1^\circ$ , then a combination of attitude angles which will satisfy this is

$$\phi_{\max} = \theta_{\max} = 0.07^\circ, \quad \psi_{\max} = 0.2^\circ$$

Take, for example, a 900-kg satellite experiencing solar pressure torque components

$$T_X = 2(1 - 2 \sin \omega_0 t) \times 10^{-5} \text{ N-m} \quad (4a)$$

$$T_Y = 10^{-4} \cos \omega_0 t \text{ N-m} \quad (4b)$$

$$T_Z = -5 \times 10^{-5} \cos \omega_0 t \text{ N-m} \quad (4c)$$

Combining equation sets (1) and (4) leads to immediate integration. If all initial rates are taken as zero, the resulting equations (in the International System of Units) are

$$\phi(t) = \phi_0 + \frac{2 \times 10^{-5}}{I_X} \left[ \frac{t^2}{2} + \frac{2}{\omega_0^2} \sin \omega_0 t - \frac{2t}{\omega_0} \right] \quad (5a)$$

$$\theta(t) = \theta_0 + (10^{-4} / \omega_0^2 I_Y) (1 - \cos \omega_0 t) \quad (5b)$$

$$\psi(t) = \psi_0 - (5 \times 10^{-5} / \omega_0^2 I_Z) (1 - \cos \omega_0 t) \quad (5c)$$

where it is assumed that  $\omega_0 = 7.28 \times 10^{-5}$  rad/sec and inertia values  $I_X = I_Z = 2000 \text{ kg-m}^2$  and  $I_Y = 440 \text{ kg-m}^2$ . Equations

(5) are used with (3) to determine values of  $t_A$  once  $\phi_{\max}$ ,  $\theta_{\max}$ , and  $\psi_{\max}$  are specified. Since  $\phi$ ,  $\theta$ , and  $\psi$  vary about the orbit, there is a range of values for  $t_A$  corresponding to each axis. The time between impulses is only  $2t_A$ . Approximate calculations indicate that this time varies from several minutes to an hour with corresponding impulses of  $10^{-3}$  to  $10^{-2} \text{ N-sec}$  for moment arms of 0.9 m. Such impulse bit sizes are well within pulsed-plasma thruster technology and should be available through beam deflection techniques.

### Minimum Thruster Component Schemes

It is now appropriate to discuss schemes which minimize the number of thrusters while satisfying satellite constraints. Toms and Kalensher<sup>2</sup> had proposed the use of a single radially oriented thruster which is mechanically vectored for all orbit and attitude functions. King and Schnelker<sup>3</sup> suggest a 3-thruster arrangement with electrostatic thrust vectorizing for attitude control. However, their north-south ( $N-S$ ) engines are not canted and only east or west drift can be controlled directly. Furthermore, the use of mechanical linkages is undesirable for long-life satellites. When potential thruster technology advances are brought into view, mission requirements may be fulfilled with as few as three fixed thrusters which have vectoring capability. The control system is assumed to have the following properties: a) the ability to apply torque components at all times, b) no momentum devices, c) no mechanical moving parts, and d)  $N-S$  thrusters with up to  $\pm 10^\circ$  vectoring in two planes using a pulsed mode. A 900-kg satellite with thrusters placed at moment arms of 0.9 m from the center of mass is assumed for illustrative purposes.

Thrust vectoring of an electrostatic beam away from its axis is now feasible. The ability to vector this beam about its axis might provide an axial torque component for each thruster. If the magnitude of this torque is sufficient, further significant hardware reductions are possible. Consider a system with the absolute minimum number of thrusters. Although a 1-thruster system is highly desirable, all attitude and orbit functions cannot be provided without mechanically maneuvering the unit. The next most desirable system is a 2-thruster arrangement. Such a scheme seems feasible if full beam vectoring potential is available. Figure 2 illustrates the thruster arrangement. Sites have been selected on the basis of arguments presented in Ref. 1. A cant angle of  $30^\circ$  is assumed for efficient use of propellant and minimal impingement problems with solar arrays. Twelve-hour thrust intervals for latitude maintenance at this cant angle require a minimum thrust of 2 N-m if at least one north and one south engine are used. Thus, there is always at least one engine firing. Each thruster can provide 3-axis control through combinations of vectoring components. Table 1 lists the attitude functions with 3-component vectoring. Note that torsional modes are assumed to produce torques along  $S_2$  and  $N_1$ , and are labeled  $S_2 t$  and  $N_1 t$ , respectively. Since all station-keeping modes can be planned in advance, there is no need for continuous east-west ( $E-W$ ) control, and  $N-S$  thrusters can be sequenced according to perturbation levels. Pitch and yaw modes result in  $E-W$  perturbations, which may be eliminated when switching between  $N_1$  and  $S_2$  engines by simultaneous thrusting with vectoring into the east or west direction. The  $30^\circ$  cant angle requires a ratio of torsional-to-plane vectoring torques of 1.73 for pitch and 0.578 for yaw to produce moments along these axes. Figure 3 illustrates combinations of the torquing modes listed in Table 1. Note that  $S_2 t = 0.55 \times 10^{-3} \text{ N-m}$  for pitch and  $0.184 \times 10^{-3} \text{ N-m}$  for yaw when  $\pm 10^\circ$  planar vectoring is used.

Applying correction torques about the  $Y$  or  $Z$  axis separately with maximum planar vectoring ( $\pm 10^\circ$ ) results in high torsional torque requirements. This technique is not necessary, although it may slightly reduce sensor logic requirements. If perturbations are interpreted along the thruster axis and transverse to it instead of along the  $Y$  and  $Z$

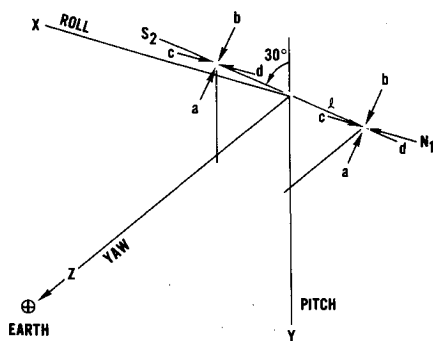


Fig. 2 Thruster orientation and nomenclature for 2-unit arrangement.

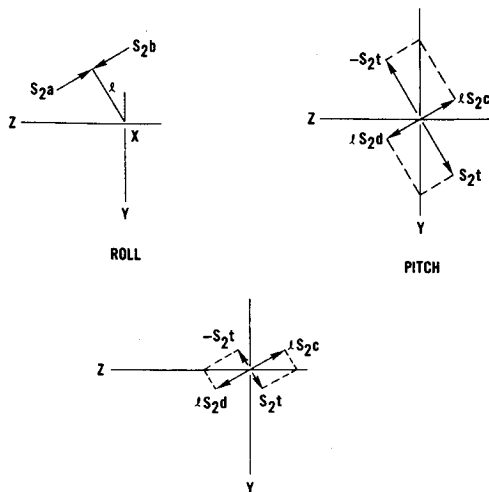


Fig. 3 Three components of torque with S2 thruster.

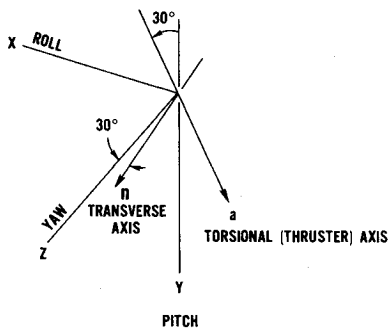


Fig. 4 Resolution of solar torque components into N-S thruster frame.

axes, then torsional torque levels for corrections are greatly reduced. The solar perturbing torque for this body-stabilized spacecraft is given by Eqs. (4). With a 30° cant angle as shown in Fig. 4, the axial (*a*) and transverse (*n*) components of pitch and yaw torques become

$$T_a = 1.1 \times 10^{-4} \cos \omega_0 t \text{ N-m}$$

$$T_n = 6.7 \times 10^{-6} \cos \omega_0 t \text{ N-m}$$

Note that  $T_x$  is not affected. Torsional torque magnitude of an electron-bombardment thruster can be approximated by

$$T_{\text{tor}} = RF\theta/2$$

where *R* is the radius of thrusting area, *F* is the thrust, and  $\theta$  is the beam deflection angle at the circumference. For a 2-N-m

Table 1 Three-component vectorable thruster operating modes

Function	Combinations	Torque magnitude <sup>a</sup>	
Roll	+	$\ell S_2 a$ or $\ell N_1 b$	$0.318 \times 10^{-3} \text{ N-m}$
	−	$\ell S_2 b$ or $\ell N_1 a$	
Pitch	+	$(S_2 t + \ell S_2 d)$	$0.626 \times 10^{-3} \text{ N-m}$
		or	
	+	$(-N_1 t + \ell N_1 c)$	
	−	$(-S_2 t + \ell S_2 c)$	
	−	$(N_1 t + \ell N_1 d)$	
Yaw	+	$(-S_2 t + \ell S_2 d)$	$0.366 \times 10^{-3} \text{ N-m}$
		or	
	+	$(N_1 t + \ell N_1 c)$	
	−	$(N_1 t + \ell N_1 c)$	
	−	$(S_2 t + \ell S_2 c)$	
North		$N_1$	
South		$S_2$	
East		$N_1 d + S_2 d$	
West		$N_1 c + S_2 c$	

<sup>a</sup>Based on 10° planar vectoring with 2-N-m thrusters.

device with 6-cm diameter and  $\theta$  value of 10°

$$T_{\text{tor}} = 5.2 \times 10^{-6} \text{ N-m}$$

Unfortunately, this is two orders of magnitude below that required for effective control of  $T_a$ . The other disturbing component  $T_n$  is easily corrected with planar vectoring.

It should be apparent at this point that two thrusters will not satisfy all requirements unless torsional vectoring can be developed well beyond expectations. Thus, at least three thrusters appear to be the minimum number feasible for complete control. Figure 5 shows engine orientations for this case. Again 12-hr thrusting is assumed with 2-N-m engines at 30° cant angles. Thruster modes for all functions are listed in Table 2. It is apparent that pitch and yaw modes are impractical with this scheme because three components of torque cannot be produced with a single engine. Hence, two thrusters are required to provide torque about these axes. East-west

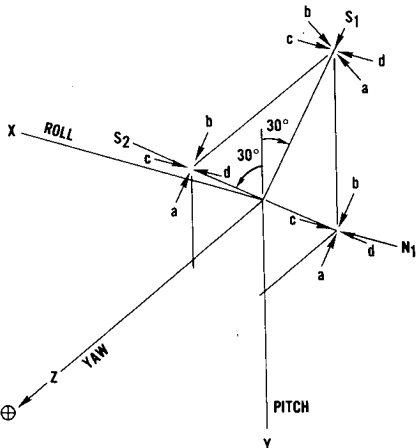


Fig. 5 Thruster orientation and nomenclature for 3-unit arrangement.

**Table 2 Two-component vectorable thruster operating modes<sup>a</sup>**

Function	Combinations
Roll	
+	$\ell S_2 a$ or $\ell N_1 b$ or $\ell S_1 b$
-	$\ell S_2 b$ or $N_1 a$ or $\ell S_1 a$
Pitch	
+	$(\ell S_1 c + \ell S_2 d)$ or $(\ell S_1 c - \ell N_1 c)$
-	$(\ell S_1 d + \ell S_2 c)$ or $(\ell S_1 d + \ell N_1 d)$
Yaw	
+	$(\ell S_1 d + \ell N_1 c)$ or $(\ell S_1 c - \ell S_2 c)$
-	

<sup>a</sup>Torque magnitude =  $0.318 \times 10^{-3}$  N-m based on  $\pm 10^\circ$  planar vectoring with 2 mN thrusters.

corrections can again be accomplished by overlapping duty cycles when switching between  $N_1$  and  $S_2$ . The logical solution to the problem of pitch and yaw control is the elimination of the  $S_1$  thruster and the addition of four pulsed-mode attitude thrusters such as the Teflon pulsed-plasma units selected in Ref. 1. The mass of each is assumed to be 5 kg. Thus, the total propulsion system mass is estimated to be 50.4 (111 lbm). However, full redundancy is not yet provided. This can be accomplished by adding  $S_1$  and  $N_2$  thrusters plus plumbing and four more Teflon units. The total mass is then about 76 kg (167 lbm) for a 10-year life with full backup capability. Further optimization should reduce this mass significantly.

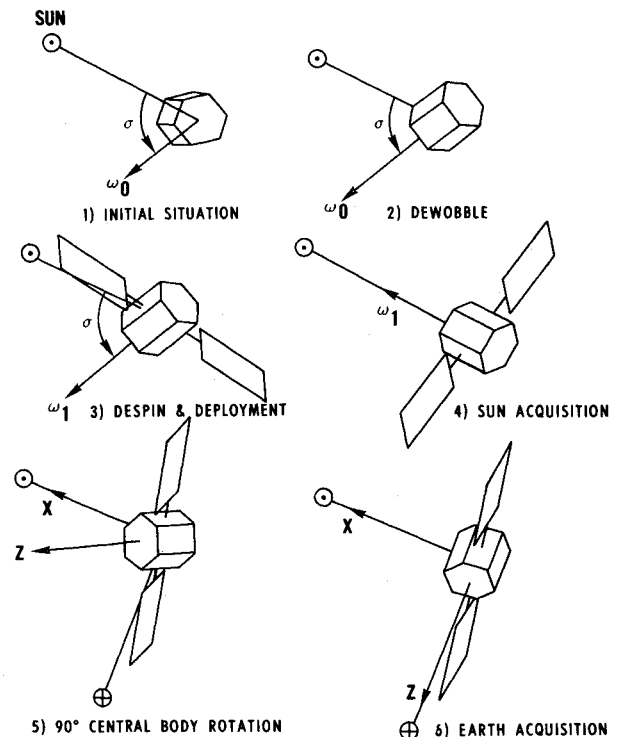
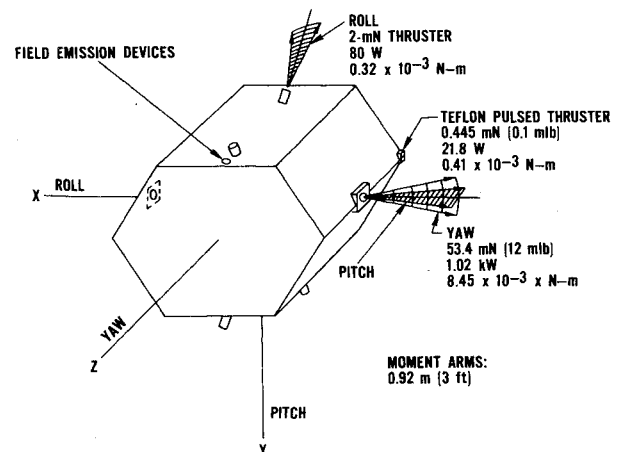
### Attitude Acquisition

Attitude acquisition maneuvers were previously recognized as critical control system sizing and configuration factors for all-thruster satellites.<sup>1</sup> A basic acquisition sequence is shown in Fig. 6. For this sequence, initial despin can be executed effectively in a matter of seconds with yo-yo devices if inertias are well-known in advance. A residual spin of  $1^\circ/\text{sec}$  is left to provide stability while initial conditions for low-torque maneuvers are established. Yo-yo devices may introduce some wobble motion if only one mass is used or if the principal inertia axes are slightly misaligned. Such wobbling will dissipate into steady spin through energy dissipation mechanisms. This situation can be corrected quickly through application of torque, or slowly through passive dissipation. Rate or rate-integrating gyros are essential to determine wobble state, control the despin maneuver, and establish an earth acquisition spin rate about the  $X$  axis. Once earth enters the sensor field of view, despin must commence to execute capture. Angular rates drop below the gyro sensitivity range, requiring earth acquisition to be completed before the earth leaves this field of view. Although solar pressure and gravity gradient torques will be active during acquisition maneuvers, attitude thruster torques will always be much greater than these torques. The maximum magnitude of gravity torque is about  $0.2 \times 10^{-4}$  N-m, which does not exceed that of solar torque.

Attitude torques may be produced by dedicated attitude thrusters, thrust vectoring of station control engines, or a combination of both. Figure 7 illustrates the application of both techniques and performance estimates assuming various sizes and types of thrusters. The use of station change and  $N-S$  thrusters for attitude acquisition may eliminate some attitude thrusters, but power levels are very high and propellant utilization very inefficient. Prior to panel deployment, high power levels may be available for a very limited time from eclipse batteries.

### Automatic Attitude Control

It is almost a necessity to provide automatic attitude control during nominal modes of satellite operation. Acquisition and reacquisition are assumed to be commanded sequences

**Fig. 6 Attitude acquisition sequence.****Fig. 7 Possible acquisition torque producers.**

based on ground processing of sensor information. Linearized equations of motion, including the gravity gradient contribution, are assumed here, since for nominal mode operation all angular displacements are small. The three component equations are<sup>4</sup>

$$T_X = I_X \ddot{\phi} + \alpha \phi + \beta \dot{\psi} \quad (\text{roll}) \quad (6)$$

$$T_Y = I_Y \ddot{\theta} + \delta \theta \quad (\text{pitch}) \quad (7)$$

$$T_Z = I_Z \ddot{\psi} + \gamma \psi - \beta \dot{\phi} \quad (\text{yaw}) \quad (8)$$

where  $T_X$ ,  $T_Y$ , and  $T_Z$  are disturbance torque components arising from solar pressure and thrust misalignment. No control torques are assumed as yet. Also

$$\alpha = 4\omega_0^2(I_Y - I_Z)$$

$$\beta = -(I_X - I_Y + I_Z)\omega_0$$

$$\gamma = \omega_0^2(I_Y - I_X)$$

$$\delta = 3\omega_0^2(I_X - I_Z)$$

The equations of motion now represent those of second-order systems without damping. Accurate attitude holding requirements cannot be maintained practically without fast damping of perturbations. Thus, control laws must provide artificial damping. This is achieved by using the following forms:

$$M_{Xc} = K_X(\tau_X \dot{\phi} + \phi) - \alpha \phi$$

$$M_{Yc} = K_Y(\tau_Y \dot{\theta} + \theta) - \delta \theta$$

$$M_{Zc} = K_Z(\tau_Z \dot{\psi} + \psi) - \gamma \psi$$

if it is assumed that attitude torques can be applied directly about the  $X$ ,  $Y$ , and  $Z$  body axes, respectively (that is, if a separate set of attitude thrusters is assumed). These expressions are added to the right-hand side of Eqs. (6-8) to result in

$$T_X = I_X \ddot{\phi} + K_X \tau_X \dot{\phi} + K_X \phi + \beta \dot{\psi}$$

$$T_Y = I_Y \ddot{\theta} + K_Y \tau_Y \dot{\theta} + K_Y \theta$$

$$T_Z = I_Z \ddot{\psi} + K_Z \tau_Z \dot{\psi} + K_Z \psi - \beta \dot{\phi}$$

Note that roll and yaw are coupled through a factor of  $\beta$ . Some response information can be obtained quickly through Laplace transform methods. The pitch equation is solved immediately as

$$\theta(s) = T_Y(s) / (I_Y s^2 + K_Y \tau_Y s + K_Y)$$

while roll and yaw must be handled simultaneously:

$$\begin{bmatrix} T_X(s) \\ T_Z(s) \end{bmatrix} = \begin{bmatrix} I_X s^2 + K_X \tau_X s + K_X & \beta s \\ -\beta s & I_Z s^2 + K_Z \tau_Z s + K_Z \end{bmatrix} \times \begin{bmatrix} \phi(s) \\ \psi(s) \end{bmatrix}$$

The characteristic fourth-order equation (C.E.) takes the form

$$\begin{aligned} \text{C.E.} = & I_X I_Z s^4 + (I_X K_Z \tau_Z + I_Z K_X \tau_X) s^3 \\ & + (I_X K_Z + I_Z K_X + K_X K_Z \tau_X \tau_Z + \beta^2) s^2 \\ & + K_X K_Z (\tau_X + \tau_Z) s + K_X K_Z \end{aligned}$$

If the condition

$$\beta^2 \ll [\max I_X K_Z, I_Z K_X, K_X K_Z \tau_X \tau_Z]$$

is satisfied, then the control response time is much less than the orbital period, and roll and yaw are effectively damped. Thus

$$\text{C.E.} \equiv (I_X s^2 + K_X \tau_X s + K_X) (I_Z s^2 + K_Z \tau_Z s + K_Z)$$

which represents two second-order systems with the properties

$$\omega_1 = (K_X / I_X)^{1/2}, \quad \zeta_1 = (\tau_X / 2) (K_X / I_X)^{1/2} \text{ (roll)}$$

$$\omega_2 = (K_Z / I_Z)^{1/2}, \quad \zeta_2 = (\tau_Z / 2) (K_Z / I_Z)^{1/2} \text{ (yaw)}$$

Solving for  $\phi(s)$  and  $\psi(s)$  gives

$$\phi(s) \equiv T_X(s) / (I_X s^2 + K_X \tau_X s + K_X)$$

$$\psi(s) \equiv T_Z(s) / (I_Z s^2 + K_Z \tau_Z s + K_Z)$$

For impulsive disturbance torques

$$\phi_{ss} = 0, \quad \theta_{ss} = 0, \quad \psi_{ss} = 0$$

For step disturbance torques

$$\phi_{ss} = T_X / K_X, \quad \theta_{ss} = T_Y / K_Y, \quad \psi_{ss} = T_Z / K_Z$$

If attitude control is provided through planar vectoring of  $N-S$  thrusters, only two independent control laws can be selected. For example, if  $M_T$  is the torque component normal to roll torque and is produced by vectoring, then a possible set of control moment formulas is

$$M_{Xc} = K_X(\tau_X \dot{\phi} + \phi) - \alpha \phi$$

$$M_{Yc} = M_T \sin \xi - \delta \theta$$

$$M_{Zc} = M_T \cos \xi - \gamma \psi$$

where  $\xi$  is the thruster cant angle measured from the pitch axis and  $M_T = K_T(\tau_T \dot{\theta} + \theta)$ . The equations of motion become

$$T_X = I_X \ddot{\phi} + K_X \tau_X \dot{\phi} + K_X \phi + \beta \dot{\psi} \text{ (roll)}$$

$$T_Y = I_Y \ddot{\theta} + K_T \tau_T (\sin \xi) \dot{\theta} + K_T (\sin \xi) \theta \text{ (pitch)}$$

$$T_Z = I_Z \ddot{\psi} + K_T \tau_T (\cos \xi) \dot{\theta} + K_T (\cos \xi) \theta - \beta \dot{\phi} \text{ (yaw)}$$

The coupling between roll and yaw is again assumed to be small, and solving for  $\psi(s)$  gives

$$\psi(s) = \frac{T_Z}{I_Z s^2} - \frac{T_Y}{I_Z s^2} \left[ \frac{K_T \tau_T s \cos \xi + K_T \cos \xi}{I_Y s^2 + K_T \tau_T s \sin \xi + K_T \sin \xi} \right]$$

which is unstable for all input disturbance torques of interest. This is a result of limited vectoring capability. Therefore, three components of control torque are required.

### Effects of Radial Component of North-South Thrust

For simplicity, several assumptions about mission requirements and satellite configuration and mass properties are used to develop quantitative conclusions about  $N-S$  thrusting strategies. The general configuration for this discussion is assumed to be a body-stabilized vehicle with two deployable solar arrays, as shown in Fig. 6. North-south electric thrusters may be mounted so that the thrust vector is in the yaw/pitch plane with radial components toward or away from the earth. The satellite mass is again assumed to be 900 kg. Offstation  $E-W$  drift resulting from any cause is permitted up to  $0.5^\circ$ . The cumulative  $E-W$  drift and daily cyclic motion due to the application of  $N-S$  electric thrusters were calculated for the specified satellite. Table 3 lists cant angles and thrust times assumed for 0.016  $N$  thrust levels, and Fig. 8 describes the nomenclature. Thrust intervals are centered about one of the satellite orbit/equatorial plane nodes.

Table 3 Firing times for selected thruster geometries

	Case I	Case II	Case III
Thrusting time	3 hr	3 hr	5 hr
		45 min	45 min
Cant angle (in $Y-Z$ plane) (deg)	30	45	60

The motion of a satellite with respect to a reference circular orbit can be described by Hill's equations for relative motion of proximate near-circular orbits<sup>5</sup>

$$\ddot{x} - 2n\dot{y} - 3n^2 x = f_x$$

$$\ddot{y} + 2n\dot{x} = f_y$$

$$\ddot{z} + n^2 z = f_z$$

Fig. 8 North-South thruster geometry.

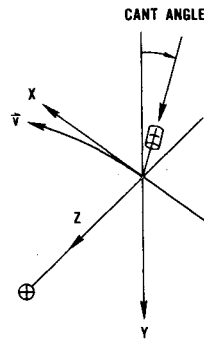


Fig. 9 Nomenclature for Hill's equations.

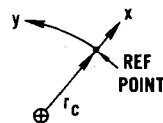


Fig. 10 Nomenclature for East-West drift calculations.

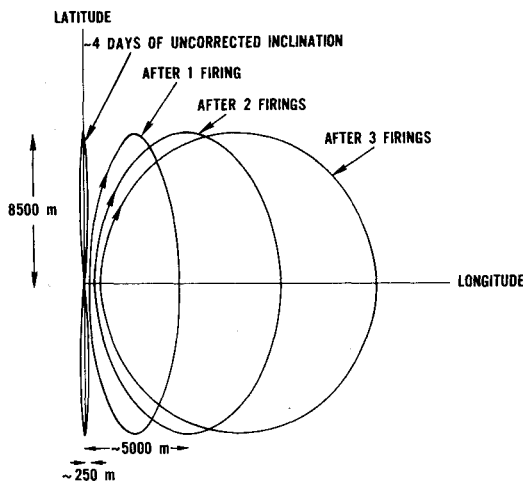
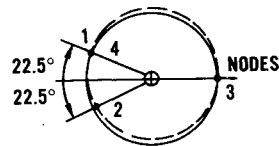


Fig. 11 Qualitative ground tracks (case I).

where  $x$  and  $y$  are defined in Fig. 9 and  $z$  is normal to the orbit plane;  $f_x$ ,  $f_y$ , and  $f_z$  are components of acceleration due to low thrust; and  $n = 7.28 \times 10^{-5}$  rad/sec for synchronous orbit. The first and second equations represent in-plane motion. Two solutions of in-plane motion are of interest here: force-free and  $f_x = \text{constant}$  cases. The former is only a special case ( $f_x = 0$ ) of the latter. Thus, only the constant radial force solution is required here. Out-of-plane motion is decoupled and can be ignored for these calculations. The  $f_x = \text{constant}$  solution is

$$x = \frac{\dot{x}_0}{n} \sin nt - \left[ \frac{f_x}{n^2} + \frac{2\dot{y}_0}{n} + 3x_0 \right] \cos nt + \left[ \frac{f_x}{n^2} + \frac{2\dot{y}_0}{n} + 4x_0 \right]$$

$$y = \frac{2\dot{x}_0}{n} \cos nt + \left[ \frac{2f_x}{n^2} + \frac{4\dot{y}_0}{n} + 6x_0 \right] \sin nt + \left[ y_0 - \frac{2\dot{x}_0}{n} \right] - \left[ \frac{2f_x}{n} + 3\dot{y}_0 + 6nx_0 \right] t$$

Table 4 Daily longitudinal displacement for selected thruster geometries

	Case I	Case II	Case III
Maximum number of thrusts	70	40	22
Longitudinal displacement per thrust (m)	262	713	2950

Rates are given by

$$\dot{x} = \dot{x}_0 \cos nt + \left[ \frac{f_x}{n} + 2\dot{y}_0 + 3nx_0 \right] \sin nt$$

$$\dot{y} = -2\dot{x}_0 \sin nt + \left[ \frac{2f_x}{n} + 4\dot{y}_0 + 6nx_0 \right] \cos nt - \left[ \frac{2f_x}{n} + 3\dot{y}_0 + 6nx_0 \right] t$$

Since the equations of motion for low-thrust cases are linear, only one orbital sequence must be computed. Superposition of subsequent orbits is then used to determine cumulative effects of radial thrust. Consider the specified situation. The sequence of calculation for case I (see Fig. 10) is as follows:

- The initial conditions at point 1 (beginning of thrust) are  $x_0 = \dot{x}_0 = y_0 = \dot{y}_0 = 0$  and  $f_x = -8.89 \times 10^{-6}$  m/sec<sup>2</sup>.
- The values of  $x$ ,  $\dot{x}$ ,  $y$ , and  $\dot{y}$  are calculated at point 2 (end of thrust). Note that  $nt_2 = 45^\circ$ .
- Let  $x_2 = x_0$ ,  $y_2 = y_0$ ,  $\dot{x}_2 = \dot{x}_0$ ,  $\dot{y}_2 = \dot{y}_0$ , and  $f_x = 0$  after point 2. The point of maximum  $y$  (point 3) is determined by setting  $\dot{y} = 0$ . Radial thrusting always leads to  $\dot{y} = 0$  at the other node, as shown. Then  $y_3$  is calculated.
- At point 4, the end of the first orbit,  $y$  is calculated.
- Finally,  $y_3$  is superimposed until  $0.5^\circ$  ( $y = 368.24$  km) is reached.

Similar procedures are used for cases II and III, and the results are summarized in Table 4. Note that during thrusting there is a drift in the direction of flight (for  $F_x < 0$ ), e.g., 262 m in 3 hr for case I. This is a direct result of the thrust interval and cant angle because the effective increase (or reduction) in gravitational pull causes an artificial decrease (or increase) in the orbit period during thrusting. Both the increasing eccentricity and this drift effect determine the maximum number of thrusts with one engine. At point 3 a maximum excursion of cyclic  $E-W$  drift occurs due to increased eccentricity. The maximum limit of  $0.5^\circ$  is reached in 70 days for case I, for example, when a nominal initial position is assumed. These maximum values may be increased by a factor of 2 by initially biasing the longitudinal position. Figure 11 shows a ground track for case I assuming some initial inclination error and longitudinal bias.

## Conclusions

Advanced design and operational aspects of zero-momentum control systems for communications satellites have been presented to the extent and depth appropriate to current interests in this concept. Considerations include duty cycle analyses, minimum thruster component configurations, attitude acquisition sequences, and automatic attitude control synthesis. No violations of mission constraints have been detected, and the overall performance appears to be very competitive. Specific conclusions concerning all-electric thruster systems include the following:

- A minimum of three thrusters will be required for complete attitude and orbit control. When reliability and redundancy are considered, this number will increase significantly.
- Three orthogonal components of control torque and continuous yaw sensing are required to insure a stable system.

c) The attitude control problem is similar for either thrust vectoring or separate attitude thruster methods.

d) Response damping must be introduced artificially through the control laws. This requires a pseudo-rate modulator to generate attitude rate information.

In addition, an important aspect of applying electric thrusters to inclination control has been exposed. Effects of a radial component of thrust indicate that alternate use of different  $N-S$  thrusters must be employed if they are canted away from the pitch axis.

### References

<sup>1</sup> Kaplan, M. H., "All-Electric Thruster Control of a Geostationary

Communications Satellite," *Journal of Spacecraft and Rockets*, Vol. 10, Feb. 1973, pp. 119-125.

<sup>2</sup> Toms, R. S. H. and Kalensher, B. E., "Control of the Attitude and Position of a Synchronous Satellite by Continuous Radial Thrust," *AIAA Journal*, Vol. 2, July 1964, pp. 1179-1188.

<sup>3</sup> King, H. J. and Schnelker, D. E., "Ion Thruster Systems with Thrust Vector Deflection," *Journal of Spacecraft and Rockets*, Vol. 8, May 1971, pp. 552-554.

<sup>4</sup> Lyons, M. G., et al., "Double Gimballed Reaction Wheel Attitude Control System for High-Altitude Communications Satellites," AIAA Paper 71-949, New York, 1971.

<sup>5</sup> Kaplan, M. H., *Modern Spacecraft Dynamics and Control*, Wiley, New York, Chap. 3; (to be published in 1976).

## *From the AIAA Progress in Astronautics and Aeronautics Series . . .*

### **GUIDANCE AND CONTROL—II—v. 13**

*Edited by Robert C. Langford, General Precision Inc., and Charles J. Mundo, Institute of Naval Studies*

This volume presents thirty-five papers on the guidance and control of missiles and space vehicles, covering active and passive attitude control for space vehicles, inertial guidance for space flight, onboard techniques for interplanetary flight, manned control of space vehicles, deep space guidance and navigation, rendezvous, and reentry and landing.

The attitude control section includes a comprehensive survey, covering a wide variety of stabilization systems for satellites, including gravity-gradient, spin, stabilization, and pulse-frequency methods. Cryostabilization studies examine drift, gyro optimization, mechanical and electrical problems, and damping. Radar and infrared studies concern sensor requirements and scanning problems.

The model and the role of the human operator in spacecraft control systems are analyzed, with emphasis on the pilot-vehicle feedback control loop. Guidance and correction algorithms and compensation are examined. Data reduction in these fields is explored.

Rendezvous studies examine Apollo program requirements, fuel-mission-orbit-thrust optimization for reentry, lunar landing, shuttle rendezvous, and orbit injection.

997 pp., 6 x 9, illus, \$24.50 Mem. & List

TO ORDER WRITE: Publications Dept., AIAA, 1290 Avenue of the Americas, New York, N. Y. 10019